International Journal of the Physical Sciences Vol. 7(6), pp. 944 - 948, 2 February, 2012
Available online at http://www.academicjournals.org/IJPS
DOI: 10.5897/IJPS11.131
ISSN 1992 - 1950 © 2012 Academic Journals

Full Length Research Paper

Effect of aging time and calcination temperature on the cerium oxide nanoparticles synthesis via reverse co-precipitation method

Marzieh Jalilpour* and Mohammad Fathalilou

Department of Mechanical Engineering, Khoy Branch, Islamic Azad University, khoy, Iran.

Accepted 23 January, 2012

In the present work, the cerium nitrate hexa-hydrate and ammonium hydroxide, used as the starting materials and the weakly agglomerated cerium oxide nanoparticles was synthesized by simple and cost effective reverse co-precipitation method. The effect of aging time and calcination temperature on structural properties of synthesized nanopowder was investigated by X-ray diffractometry (XRD), simultaneous thermal analysis (STA), Fourier transform infrared (FT-IR), scanning electron microscopy (SEM) and transmission electron spectroscopy (TEM) analytical methods. The investigation showed that aging of the precipitated precursors has pronounced effect on the decreasing of the agglomeration, increase in the crystallinity and the crystallite size of the final product obtained after calcination. Also, increase in the calcination temperature led to the appreciable increase in the crystallite size as well as the crystallinity.

Key words: Aging time, ammonium hydroxide, calcination temperature, ceria nanoparticles, reverse co-precipitation.

INTRODUCTION

Ceria (CeO_2) is a cubic fluorite-type structured ceramic material that does not show any known crystallographic change from room temperature up to its melting point (2700°C) (Corradi et al., 2006; Li et al., 2002; Hassanzadeh-tabrizi et al., 2010). In recent years, nanocrystalline cerium oxide (CeO_2) particles have been extensively studied owing to their potential uses in many applications, such as UV absorbents and filters (Cheviré et al., 2006; Souza et al., 2010), gas sensors (Izu et al., 2003; Jasinski et al., 2003), electrolytes in the fuel cell technology (Lapa et al., 2010; Matovic et al., 2009), water-gas shift catalysts (Gorte and Zhao, 2005), polishers for chemical mechanical planarization (CMP) (Xin et al., 2010; Lee et al., 2009), ceramic pigments (Llusar et al., 2010; Matovic et al., 2010), etc. Most of the applications require the use of non-agglomerated nanoparticles, as aggregated nanoparticles lead to inhomogeneous mixing and poor sinterability. However, nanocrystallites with a primary particle size <5 nm have a stronger tendency to agglomerate, making processing very difficult. Also, the benefits expected from highly crystalline nanoparticles are easily lost during the manufacture of components unless weakly agglomerated nanoparticles can be produced (Tok et al., 2007). Accordingly, preparation of ultrafine CeO_2 powders without agglomeration has been intensively investigated. CeO_2 nanopowders can be synthesized by different methods, such as, hydrothermal (Dos Santos et al., 2008), mechanochemical (Zec et al., 2009), combustion synthesis (Mukherjee et al., 2008), sol-gel (Tao et al., 2009), microemulsion (Chandradass et al., 2009), co-precipitation (Godinho et al., 2007) and spray-pyrolysis (Yao and Xie, 2007). Compared with these methods, co-precipitation method is one of the most promising techniques because of the inexpensive starting materials, a simple synthesis process with reproducible results and commonly available apparatus (Truffault et al., 2010; Hassanzadeh-tabrizi et al., 2010). Although, CeO_2 nano-particles have been extensively studied by precipitation method but most of the previous reports were focused on

*Corresponding author. E-mail: jalilpour.marzieh@gmail.com.

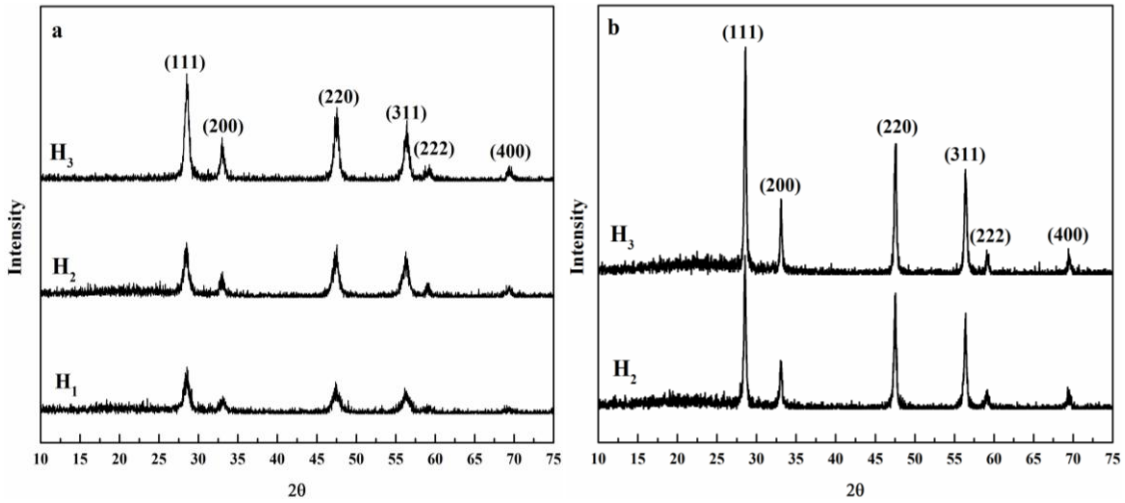

Figure 1. The X-ray diffraction pattern of ceria nanoparticles calcined at (a) 600°C and (b) 800°C.

on direct precipitation of ceria (Yamashita et al., 2002; Zhou et al., 2002; Uekawa et al., 2002).

In this work, the ceria nanoparticles were synthesized via reverse co-precipitation method, using cerium nitrate hexa-hydrate and ammonium hydroxide as precipitation agent. The purpose of this work was to investigate the aging time and calcination temperature effect on the structural characteristics of the final product.

MATERIALS AND METHODS

In this study, cerium nitrate hexa-hydrate ($Ce(NO_3)_3.6H_2O$; extra pure, Merck Chemical Company, Inc.) and ammonium hydroxide ($(NH_4)OH$; extra pure, Merck Chemical Company, Inc.) were used as the starting materials. The cerium nitrate solution with 0.1 M concentration was prepared and added dropwise at the speed of 3 to 4 ml/min into the 1 M ammonium hydroxide stirring solution until the precipitation process was completed. The suspensions were aged at room temperature for 1, 6 and 12 h, respectively and were then centrifuged to collect precursor. The precursors were then thoroughly washed 3 times with distilled water and were rinsed with ethanol, respectively. They were then dried at 80°C for 12 h and calcined at 600 and 800°C for 2 h to yield the cerium oxide nanoparticles. The synthesized samples obtained at various aging times (1, 6 and 12 h) were named $H_{1\text{-}600}$, $H_{6\text{-}600}$ and $H_{12\text{-}600}$, after calcination at 600°C and $H_{1\text{-}800}$, $H_{6\text{-}800}$ and $H_{12\text{-}800}$ after calcination at 800°C, respectively.

Phase identification was done via X-ray diffractometry (XRD) on a Philips X-ray diffractometer (PW3710) operating at 20 kV/10 mA using nickel-filtered CuKα radiation in the range of 2θ = 10 to 80°. Crystallite sizes (D_{XRD}) of the calcined powders were calculated by the X-ray line broadening technique performed on the (111) diffraction of CeO_2 lattice using the Scherrer Equation 1:

$$D_{XRD} = K\lambda / \beta \cos\theta \quad (1)$$

where θ is the Bragg angle of diffraction lines, K is a shape factor (K = 0.9 in this work), λ is the wavelength of incident X-rays (λ = 0.15406 nm) and β is the corrected half width given by Equation 2:

$$\beta^2 = {\beta_m}^2 - {\beta_s}^2 \quad (2)$$

where β_m is the measured half-width and β_s is the half width of a standard CeO_2 sample with a known crystallite size of larger than 1 ηm.

Lattice parameter of synthesized powders was calculated by Equation 3:

$$d_{(hkl)} = \frac{a}{\sqrt{h^2 + k^2 + l^2}} \quad (3)$$

Differential thermal analysis/thermogravimetry (DTA/TGA) of the dried precursors was done on a simultaneous thermal analysis (STA) analyzer (PL STA1640) in flowing air with a heating rate of 10°C min^{-1}. The α-Alumina was used as the reference material. Particle morphologies of the CeO_2 powders were observed via scanning electron microscopy (SEM) (Stereo Scan S360 and WEGA TE Scan). The microstructure, size distribution and shape of the particles were investigated with transmission electron spectroscopy (TEM) (Jeol USA and Zeiss Germany). Further structural characteristics were determined by FT-IR spectroscopy (Bruker vector33).

RESULTS AND DISCUSSION

Figure 1a and b show the powder XRD pattern of the synthesized powders after calcination at 600 and 800°C for 2 h, respectively. The diffraction peaks of all the samples assigned to cubic fluorite CeO_2 are consistent with the JCPDS file of CeO_2 (JCPDS No. 34-0394). The patterns in Figure 1a shows that increase in the aging time causes increase in the crystallinity. According to Figure 1b, at higher calcination temperature (800°C), the peaks are appreciably sharpened which indicate higher crystallinity. Also, Table 1 shows that increase in both the aging time and calcination temperature leads to appreciable grain growth in the crystallite size.

Table 1. Crystallite sizes of CeO_2 powders before and after calcinations.

Calcination temperature (°C)	Powder name	Crystallite size (nm) from (111) peak	Lattice parameter (nm) from (111) peak
600	H_1	5.9	0.5422
600	H_2	6.5	0.5420
600	H_3	7.3	0.5419
800	H_2	24.4	0.5416
800	H_3	26.8	0.5414

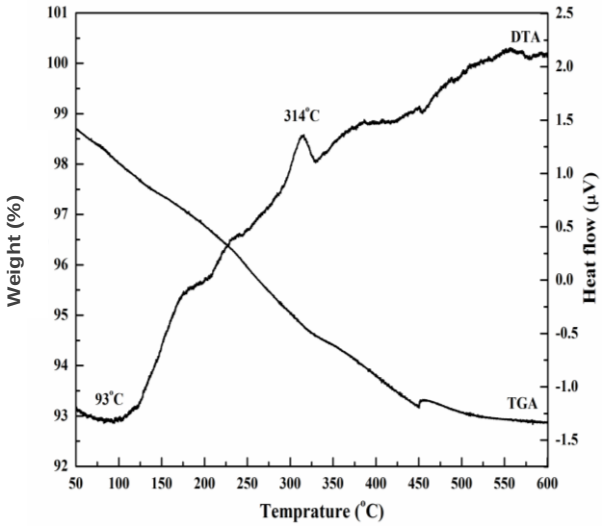

Figure 2. STA curves of H_2.

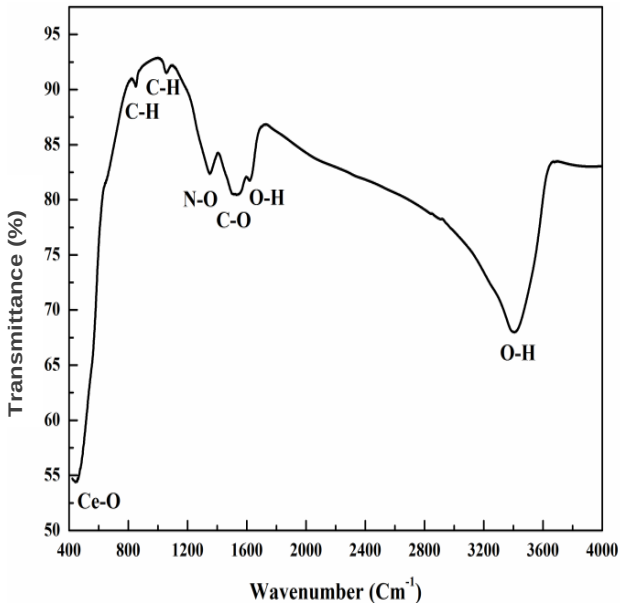

Figure 3. FT-IR spectra of CeO_2 nanoparticles with 1 h aging.

Furthermore, it can be seen that in smaller crystallite sizes, due to the presence of more point defect, the lattice parameter became greater and the expansion occurred in the crystal lattice.

Figure 2 shows the DTA-TGA curves of the co-precipitated CeO_2 precursor which was aged for 1 h. It is seen that the TGA and STA curves illustrate two stages of the calcinion process; the endothermic reaction at around 93°C and the exothermic reaction at ~314°C, due to the removal of the absorbed water and decomposition of residual nitrate, respectively (Godinho et al., 2007). In fact, STA study did not show significant processes occurring during the heating of the samples, which indicates that the formation of CeO_2 crystallites has already been taking place during precipitation and aging process.

Figure 3 displays the FT-IR spectrum of CeO_2 nanoparticles in the wave number range from 400 to 4000 cm^{-1}. The absorption bands around 3400 and 1620 cm^{-1} are attributed to the stretching mode of water and hydroxyls, respectively. A sharp band at 1385 cm^{-1} is indicative of N-O stretching vibration due to the traces of nitrate. The band at wave number below 500 cm^{-1} corresponds to the Ce-O bands (Athawale et al., 2009; Yue and Phanichphant, 2009).

Typical morphologies and agglomeration states of the nanopowders were obtained after 1 and 6 h aging observed as shown in Figure 4. It can be seen that the size of the secondary particles are ~50 and ~40 nm for H_1 (Figure 4a) and H_2 (Figure 4b) samples, respectively, consisting of the fine particles smaller than 10 nm. The SEM observations indicate increase in the results in the smaller nanoparticles with weaker agglomeration.

The crystalline size has also been directly observed using a transmission electron microscope (TEM). As shown in Figure 5, the calcined nanoparticles possess approximately spherical shape in the both of $H_{1\text{-}600}$ and $H_{2\text{-}600}$ samples. Moreover, the size distribution of the particles is uniform and the average crystallite size is ~3 and ~6 nm for H_1 and H_2, respectively, which approximately agrees with the result obtained by XRD studies, indicating a well-defined dispersing state without significant hard agglomeration.

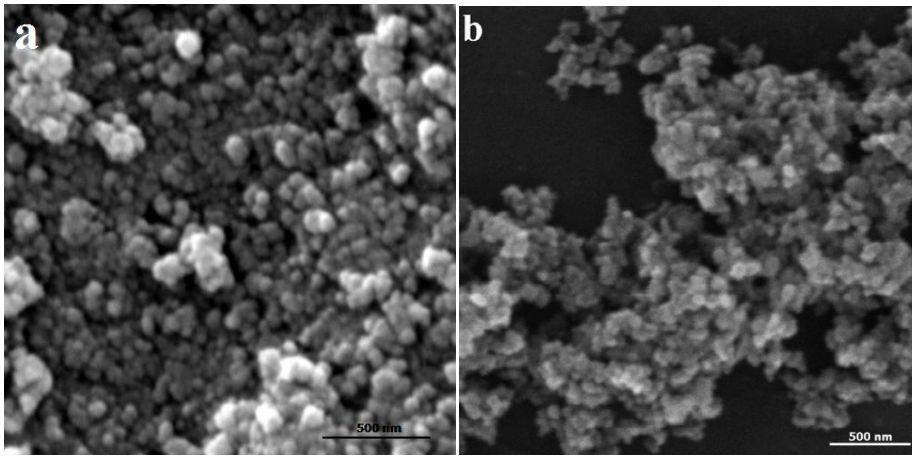

Figure 4. SEM photographs of CeO_2 powders calcined at 600°C, (a) H_1 and (b) H_2.

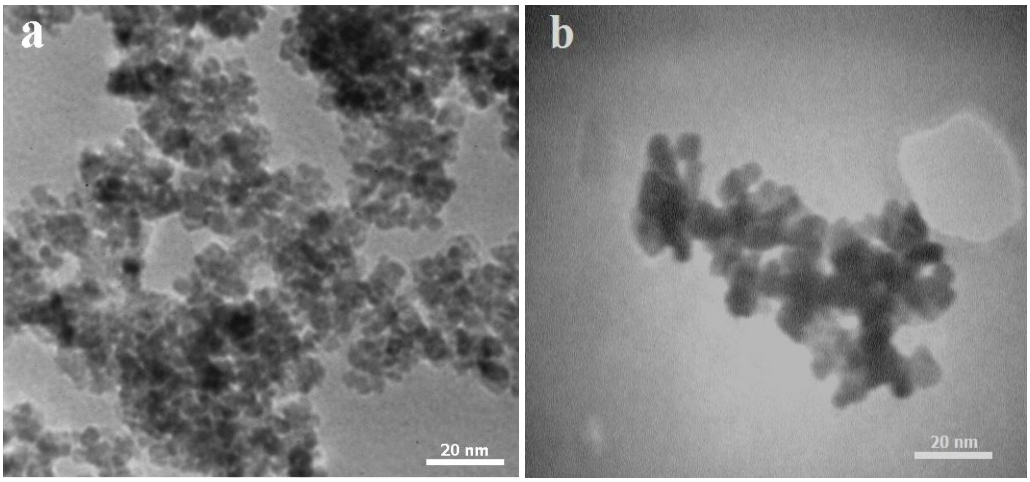

Figure 5. TEM photographs of CeO_2 powders calcined at 600°C, (a) H_1 and (b) H_2.

Conclusion

In this work, ceria nanoparticles were synthesized by simple and cost-effective reverse co-precipitation method. Effect of aging time and calcination temperature was studied, which showed that aging time influences the size and morphology of the synthesized nanoparticles, that is, increase in aging time led to larger crystallite sizes, smaller particle sizes, weaker agglomeration and more crystallinity. Also, increase in the calcination temperature resulted in higher crystallinity and much coarser crystallites.

REFERENCES

Athawale AA, Bapat MS, Desai PA (2009). Hydroxide directed routes to synthesize nanosized cubic ceria (CeO_2). J. Alloys. Compd., 484: 211–217.

Chandradass J, Nam B, Kim KH (2009). Fine tuning of gadolinium doped ceria electrolyte nanoparticles via reverse microemulsion process. Colloids Surf A: Physicochem. Eng. Asp., 348: 130–136.

Cheviré F, Munoz F, Baker CF, Tessier F, Larcher O, Boujday S, Colbeau-Justin C, Marchand R (2006). UV absorption properties of ceria-modified compositions within thefluorite-type solid solution CeO_2–Y_6WO_{12}. J. Solid State Chem., 179: 3184–3190.

Corradi AB, Bondioli F, Ferrari AM, Manfredini T (2006). Synthesis and characterization of nanosized ceria powders by microwave–hydrothermal method. Mater. Res. Bull., 41: 38–44.

Dos Santos ML, Lima RC, Riccardi CS, Tranquilin RL, Bueno PR, Varela JA, Longo E (2008). Preparation and characterization of ceria nanospheres by microwave-hydrothermal method. Mater. Lett., 62: 4509–4511.

Godinho MJ, Gonçalves RF, Santos LPS, Varela JA, Longo E, Leite ER (2007). Room temperature co-precipitation of nanocrystalline CeO_2 and $Ce_{0.8}Gd_{0.2}O_{1.9-\delta}$ powder. Mater. Lett., 61: 1904–1907.

Gorte RJ, Zhao S (2005). Studies of the water-gas-shift reaction with ceria-supported precious metals. Catal. Tod., 104: 18–24.

Hassanzadeh-Tabrizi SA, Mazaheri M, Aminzare M, Sadrnezhaad SK (2010). Reverse precipitation synthesis and characterization of CeO_2 nanopowder. J. Alloys Compd., 491: 499–502.

Izu N, Shin W, Murayama N (2003). Fast response of resistive-type oxygen gas sensors based on nano-sized ceria powder. Sens.

Actuators B., 93: 449–453.
Jasinski P, Suzuki T, Anderson HU (2003). Nanocrystalline undoped ceria oxygen sensor. Sens. Actuators B., 95: 73–77.
Lapa CM, de Souza DPF, Figueiredo FML, Marques FMB (2010). Two-step sintering ceria-based electrolytes. Int. J. hydrogen energy, 35: 2737–2741.
Li J, Ikegami T, Wang Y, Mori T (2002). Nanocrystalline $Ce_{1-x}Y_xO_{2-x/2}$ ($0 \le X \le 0.35$) Oxides via Carbonate Precipitation: Synthesis and Characterization. J. Solid State Chem., 168: 52–59.
Llusar M, Vitaskova L, Sulcova P, Tena MA, Badenes JA, Monros G (2010). Red ceramic pigments of terbium-doped ceria prepared through classical and non-conventional coprecipitation routes. J. Euro. Cer. Sci., 30: 37–52.
Matovic B, Boskovic S, Logar M, Radovic M, Dohcevic-Mitrovic Z, Popovic ZV, Aldinger F (2010). Synthesis and characterization of the nanometric Pr-doped ceria. J. Alloys Compd., 505: 235–238.
Matovic B, Dohcevic-Mitrovic Z, Radovic M, Brankovic Z, Brankovic G, Boskovic S, Popovic ZV (2009). Synthesis and characterization of ceria based nanometric powders. J. Power Sour., 193: 146–149.
Mukherjee ST, Bedekar V, Patra A, Sastry PU, Tyagi AK (2008). Study of agglomeration behavior of combustion-synthesized nano-crystalline ceria using new fuels. J. Alloys Compd., 466: 493–497.
Souza ECC, Brito HF, Muccillo ENS (2010). Optical and electrical characterization of samaria-doped ceria. J. Alloys Compd., 491: 460–464.
Tao Y, Shao J, Wang J, Wang WG (2009). Morphology control of $Ce_{0.9}Gd_{0.1}O_{1.95}$ nanopowder synthesized by sol–gel method using PVP as a surfactant. J. Alloys Compd., 484: 729–733.
Tok AIY, Boey FYC, Dong Z, Sun XL (2007). Hydrothermal synthesis of CeO_2 nano-particles. J. Mater. Proc. Technol., 190: 217–222.
Truffault L, Ta M, Devers T, Konstantinov K, Harel V, Simmonard C, Andreazza C, Nevirkovets IP, Pineau A, Veron O, Blondeau JP (2010). Application of nanostructured Ca doped CeO_2 for ultraviolet filtration. Mater. Res. Bull., 45: 527–535.
Uekawa N, Ueta M, Wu YJ, Kakegawa K (2002). Characterization of CeO_2 Fine Particles by Homogeneous Precipitation Method with Polyethylene Glycol. Chem. Lett., 8: 854–855.
Xin J, Cai W, Tichy JA (2010). A fundamental model proposed for material removal in chemical–mechanical polishing. Wear, 268: 837–844.
Yamashita M, Kameyama K, Yabe S, Yoshida S, Fujishiro Y, Kawai T, Sato T (2002). Synthesis and microstructure of calcia doped ceria as UV filters. J. Mater. Sci., 37: 683–687.
Yao SY, Xie ZH (2007). Deagglomeration treatment in the synthesis of doped-ceria nanoparticles via coprecipitation route. J. Mater. Proc. Technol., 186: 54–59.
Zec S, Boskovic S, Kaluderovic B, Bogdanov Z, Popovic N (2009). Chemical reduction of nanocrystalline CeO_2. Cer. Int., 35: 195–198.
Zhou XD, Huebner D, Anderson HU (2002). Size-induced lattice relaxation in CeO_2 nanoparticles. Appl. Phys. Lett., 80: 3814–3816.